

# 1 **Disconnect between Hadley Cell and Subtropical Jet variability** 2 **and response to increased CO<sub>2</sub>**

3 **Molly E. Menzel<sup>1</sup>, Darryn Waugh<sup>1,2</sup>, Kevin Grise<sup>3</sup>**

4 <sup>1</sup>Department of Earth and Planetary Sciences, Johns Hopkins University, Baltimore, Maryland, USA

5 <sup>2</sup>School of Mathematics, University of New South Wales, Sydney, New South Wales, Australia

6 <sup>3</sup>Department of Environmental Sciences, University of Virginia, Charlottesville, Virginia, USA

## 7 **Key Points:**

- 8 • CMIP5 analysis shows the subtropical jet (STJ) latitude does not co-vary interannu-  
9 ally with the Hadley Cell (HC) edge but the STJ strength does moderately.
- 10 • The interannual relationship between HC edge and STJ strength is the opposite sign  
11 as the response to increased atmospheric CO<sub>2</sub>.
- 12 • The differences in the HC-STJ relationship are related to the differing sensitivities  
13 of the HC and STJ to shifts in eddy momentum fluxes.

---

Corresponding author: Molly Menzel, [molly.menzel@jhu.edu](mailto:molly.menzel@jhu.edu)

## Abstract

The subtropical jet (STJ) is thought to co-exist with the edge of the Hadley cell (HC). However, recent studies reveal that the location of the STJ is poorly correlated with the latitude of the poleward edge of the HC. Here we use output from the Coupled Model Intercomparison Project phase 5 (CMIP5) to show that a weaker STJ is associated with a more poleward HC edge interannually, but there is a strengthening of the STJ and expansion of the HC in response to increased CO<sub>2</sub>. The HC expansion caused by increased CO<sub>2</sub> is much more rapid than the strengthening of the STJ. It is suggested that the differing response times and relationships between interannual variations and increased CO<sub>2</sub> are due to differing sensitivities of the HC and STJ to shifts in the eddy momentum fluxes.

## 1 Introduction

The existence of the subtropical jet (STJ) is generally attributed to angular momentum transport within the Hadley Cell (HC) [Kim and Lee, 2004], and axisymmetric theory predicts the location of a STJ at the poleward edge of the HC [Held and Hou, 1980]. A STJ at the HC edge is indeed found in reanalyses and climate models. However, several recent studies have shown that, even though there is strong relationship between the variability of locations of the HC edge and eddy-driven jet (EDJ), there is little relationship between variability in the edge of the HC and the latitude of STJ [Solomon *et al.*, 2016; Davis and Birner, 2017; Waugh *et al.*, 2018]. Specifically, even though their climatological latitudes are similar, there are very weak interannual correlations between the latitude of the HC edge and STJ, over both hemispheres and for all seasons. Furthermore, while the HC expands in simulations with increasing CO<sub>2</sub>, there is no consistent change in the STJ latitude [Davis and Birner, 2017; Waugh *et al.*, 2018; Wang *et al.*, 2018].

This disconnect between movement of the STJ and HC edge is surprising, and suggests a gap in our understanding of the dynamics of the STJ. Understanding the variability and trends of the STJ is important, as its location has been used as a metric for tropical width [Fu and Lin, 2011; Archer and Caldeira, 2008; Manney and Hegglin, 2018]. Moreover, the STJ is a key component of the global atmospheric circulation and influences numerous atmospheric processes including subtropical cyclogenesis [Otkin and Martin, 2004], atmospheric rivers and other extreme events [Ryoo *et al.*, 2013; Zhang and Villarini, 2018; Winters and Martin, 2014], and wave propagation between the tropics and extratrop-

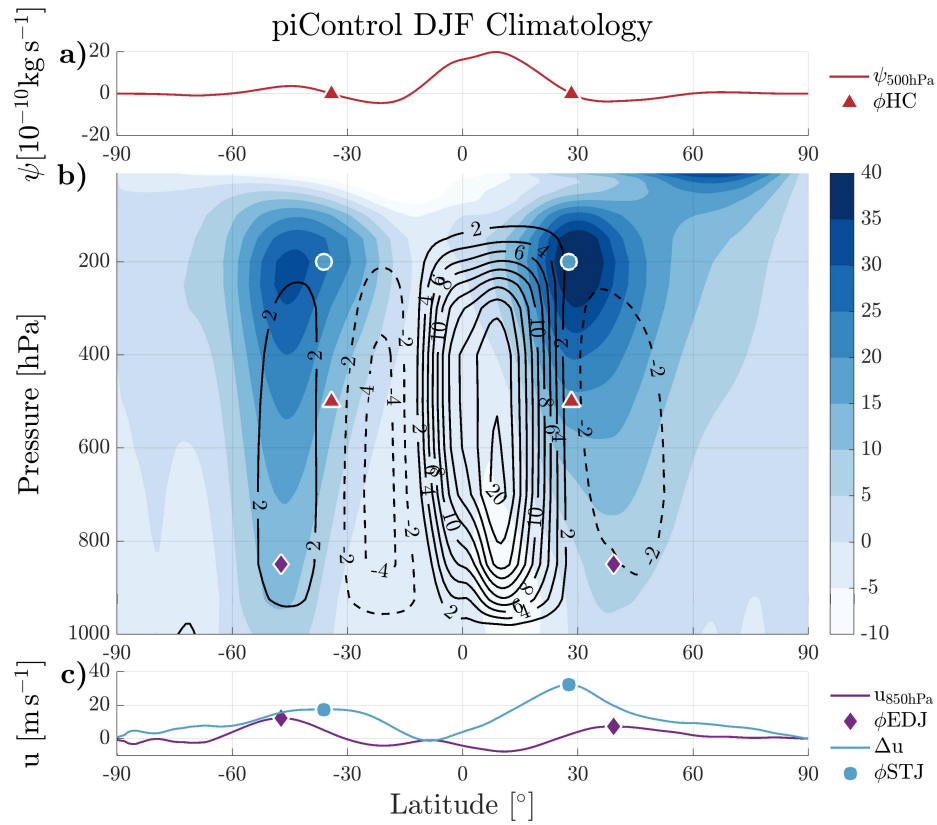
45 ics [Mathews and Kiladis, 1999], between hemispheres [Webster and Holton, 1982], and  
46 into the stratosphere [Shepherd and McLandress, 2011].

47 In this study we further examine the HC-STJ relationship by considering the intensi-  
48 ties of the HC and STJ, in addition to the latitudes of the STJ and HC edge. We examine  
49 both the natural variability and forced response of the HC and STJ in a large number of  
50 climate models, and investigate the mechanisms causing variability and trends in the two  
51 features. We find that the HC edge and STJ strength relationship reverses sign between in-  
52 terannual variability and the response to increased atmospheric CO<sub>2</sub>. It is suggested that  
53 this is due to the differing sensitivities of the HC edge and STJ strength to shifts in lat-  
54 itude of the peak eddy momentum flux, which would be consistent with previous work  
55 showing the HC edge’s response to increased CO<sub>2</sub> is closely connected to changes in the  
56 midlatitudes [Chemke and Polvani, 2019; Shaw and Tan, 2018], while the STJ is more in-  
57 fluenced by the tropics [Shaw and Tan, 2018].

## 58 2 Data and Methods

59 Our analysis is performed using monthly-mean model output from 23 climate mod-  
60 els that participated in the Coupled Model Intercomparison Project, Phase 5 (CMIP5)  
61 [Taylor et al., 2012]. These are the same models as those considered in Grise and Polvani  
62 [2017] and Waugh et al. [2018] (see Supporting Information, Table S1). As in these stud-  
63 ies, we analyze the first ensemble member (“r1i1p1”) from the preindustrial control (pi-  
64 Control) and the instantaneous quadrupling of atmospheric CO<sub>2</sub> (4xCO<sub>2</sub>) simulations. The  
65 analysis of the control simulations gives insight into the system’s natural variability (Sect.  
66 3) whereas the changes in the 4xCO<sub>2</sub> simulations relative to the control allow us to evalu-  
67 ate the response of the HC and STJ to increased radiative forcing (see Sect. 4).

74 To quantify the characteristics of the HC and STJ, we use metrics calculated us-  
75 ing the Tropical-width Diagnostics (TropD) code [Adam et al., 2018]. The zonal-mean  
76 fields used to define these metrics are presented in Figure 1 which shows the DJF clima-  
77 tology. For all calculations, the basic fields are zonally and temporally averaged (i.e. over  
78 a season) before calculation of the metrics. The edge of the HC ( $\phi_{HC}$ ) is defined as the  
79 latitude at which the mean meridional streamfunction at 500 hPa ( $\psi_{500}$ ) crosses zero pole-  
80 ward of its tropical extremum (Fig. 1a), and is calculated using the “Psi\_500” method in  
81 TropD\_Metric\_PSI.



68 **Figure 1.** CMIP5 multi-model mean DJF climatology of (a) mean meridional circulation at 500 hPa, (b)  
 69 zonal-mean zonal wind (blue contours, in units of  $\text{m s}^{-1}$ ) and mean meridional circulation (black contours  
 70 such that solid and dashed lines denote clockwise and counter-clockwise direction respectively, in units  
 71  $10^{10} \text{kg s}^{-1}$ ), and (c) zonal-mean zonal wind at 850 hPa (purple) and the change in wind between the upper  
 72 troposphere and 850 hPa (blue) for the piControl simulation. Locations of the HC edge, EDJ, and STJ are  
 73 noted by the red triangle, purple diamond, and blue circle, respectively.

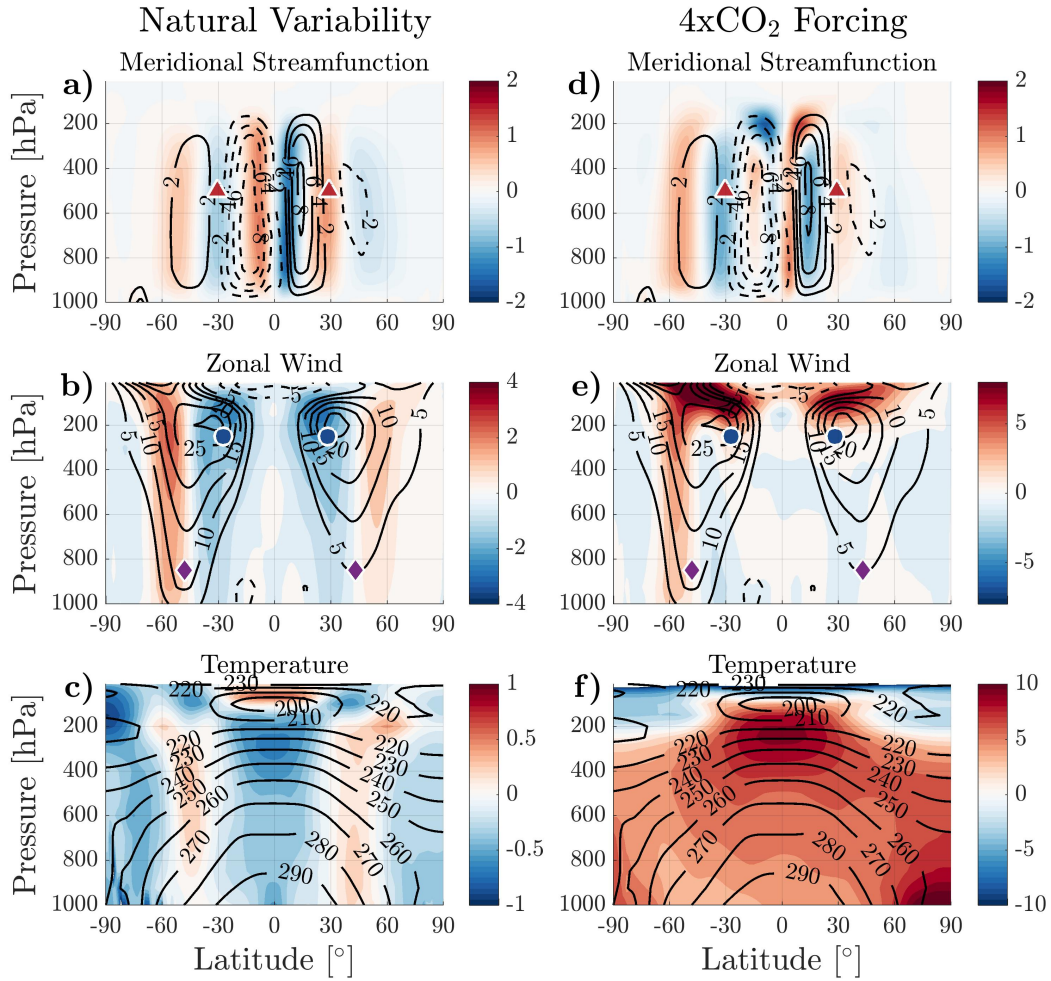
82 The latitude of the STJ ( $\phi_{STJ}$ ) is the latitude of maximum  $\Delta u$ , where  $\Delta u$  subtracts  
 83 the near-surface zonal-mean wind at 850 hPa from the column integrated zonal-mean up-  
 84 per tropospheric wind between 100-400 hPa (Fig. 1c). Defining the STJ based on  $\Delta u$   
 85 (referred to as the “adjusted method” [Adam *et al.*, 2018]) enables a better distinction of  
 86 the STJ from the eddy-driven jet (EDJ) [Davis and Birner, 2016] than by simply finding  
 87 the latitude of maximum column integrated zonal-mean tropospheric wind between 100-  
 88 400 hPa (referred to as the “core method” [Adam *et al.*, 2018]). In seasons where the STJ  
 89 is well separated from the EDJ (e.g., during winter [Lachmy and Harnik, 2014; Eichel-  
 90 berger and Hartmann, 2007; Lee and Kim, 2003]), the two methods detect the STJ at a  
 91 similar latitude around 30°, sufficiently distinct from the EDJ (see Supporting Information,  
 92 Figure S1). However, in the seasons that have a relatively weak subtropical jet (such as  
 93 summer), the core method produces a STJ that is noticeably poleward from the adjusted  
 94 STJ and located next to the EDJ (see Supporting Information, Figure S1). In this case,  
 95 the core method is mistaking the EDJ for the STJ. For this reason, the adjusted method  
 96 is a more accurate tool for locating the STJ, even though the STJ is not entirely isolated  
 97 from the impact of eddies [Lee and Kim, 2003]. In Waugh *et al.* [2018],  $\phi_{STJ}$  was calcu-  
 98 lated using the “adjusted\_max” method in TropD\_Metric\_STJ, but here we use a quadratic  
 99 “fit” method to find the latitude of the maximum value, making it easier to determine the  
 100 strength of the STJ (see below).

101 Additionally, we define metrics to quantify the strength of the HC and STJ. The  
 102 strength of the HC ( $max_{HC}$ ) is calculated as the maximum value of  $\psi_{500}$  inside the HC  
 103 (between the equator and  $\phi_{HC}$ ), while the STJ strength ( $max_{STJ}$ ) is the magnitude of  $\Delta u$   
 104 at  $\phi_{STJ}$ , the maximum value of the quadratic fit.

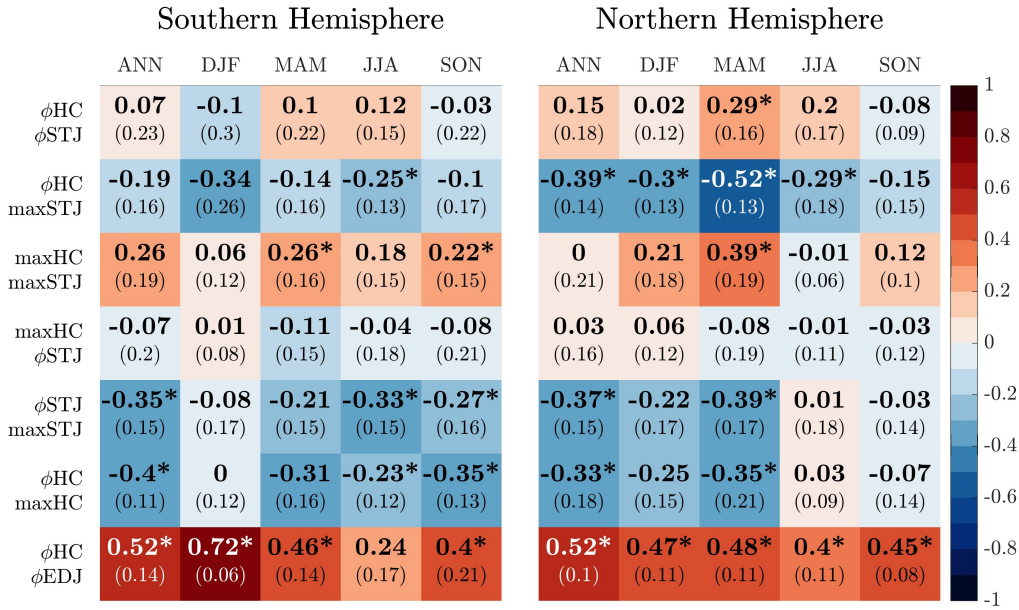
105 The latitude of the EDJ ( $\phi_{EDJ}$ ) is the latitude of maximum zonal-mean 850 hPa  
 106 zonal winds ( $u_{850}$ , Fig. 1c), and is calculated in TropD\_Metric\_EDJ using the same quadratic  
 107 fit method as  $\phi_{STJ}$ .

### 108 3 Interannual Variability

117 We first examine the interannual variability of the HC and STJ in the control runs  
 118 of the models. Before considering the correlations between different metrics, we exam-  
 119 ine how the zonal-mean meridional circulation, zonal wind, and temperature vary with a  
 120 change in the width of the HC (Fig. 2a-c). The left hand plots in Figure 2 show the multi-



109 **Figure 2.** Zonally averaged, multi-model, annual-mean climatologies (black contours) and changes (colored  
 110 shading) in (top) mean meridional streamfunction ( $10^{10} \text{ kg s}^{-1}$ ), (middle) zonal wind ( $\text{m s}^{-1}$ ), and (bottom)  
 111 temperature (K) due to (a-c) natural variability and (d-f)  $4\text{xCO}_2$ . Note the color scales are different for each  
 112 plot. Here, the change due to natural variability is calculated by composites of an expanded HC ( $\phi\text{HC}$  more  
 113 poleward than  $2\sigma$ ) minus a contracted HC ( $\phi\text{HC}$  more equatorward than  $2\sigma$ ) and the change due to  $4\text{xCO}_2$  is  
 114 the response averaged over years 100-150 after applied forcing minus the control climatology. Climatological  
 115 locations of the HC edge, EDJ, and STJ from piControl are noted by the red triangle, purple diamond, and  
 116 blue circle, respectively.



134 **Figure 3.** Model-mean correlations (bold, colored) and standard deviations of model spread (in paren-  
 135 theses) for various metric relationships. An asterisk denotes that at least 20 of the 23 models' correlations  
 136 are statistically significant at a 95% confidence level. Correlations were calculated for control simulations to  
 137 represent the metrics' natural variability.

121 model, annual-mean difference between composites of an expanded and contracted HC  
 122 for each of these fields. We consider the HC to be expanded or contracted when  $\phi$ HC is  
 123 poleward or equatorward of its climatological mean value by more than two standard de-  
 124 viations, respectively, corresponding to about  $0.9^\circ$  latitude. When the HC is expanded, it  
 125 is weaker by up to  $0.5 \times 10^{10} \text{ kg s}^{-1}$  (Fig. 2a), and there is a strengthening of surface winds  
 126 on poleward side of the mid-latitude jet, consistent with the well documented poleward  
 127 shift of the EDJ when there is a broader HC (Fig. 2b). In the upper troposphere there is a  
 128 weakening of the zonal winds in the subtropics by  $\sim 20\text{-}30\%$  and a narrow tropical cool-  
 129 ing (Fig. 2c). Altogether, Fig. 2a-c demonstrate that a weakening of the HC, poleward  
 130 shift of the EDJ, a narrow tropical cooling and a weakening of the STJ are related to a  
 131 HC expansion. The changes in the HC, EDJ and tropical temperatures shown in Fig. 2a-  
 132 c are very similar to the difference between La Niña and El Niño events [e.g., *Lu et al.*,  
 133 2008].

138 To better quantify the relationships shown in Fig. 2a-c, we use the metrics described  
 139 in Section 2 to statistically evaluate the natural co-variability of the HC with the STJ.

140 Figure 3 presents correlations between the various metrics for each season and hemi-  
 141 sphere. The correlations, shown in bold and corresponding to the shading of each square,  
 142 were calculated in time for each model and then averaged across models. The numbers in  
 143 parentheses under the correlations in Fig. 3 are the standard deviations of the correlations  
 144 across models, indicating model spread in correlation values, and the asterisk denotes that  
 145 at least 20 of the 23 models' correlations are significant at the 95% confidence level.

146 As shown in previous studies, Figure 3 shows there are almost no significant corre-  
 147 lations between the HC edge and the STJ location (Fig. 3, row 1), a surprising result that  
 148 contrasts the well known strong, positive correlation between the HC edge and latitude of  
 149 the EDJ during most seasons (Fig. 3, row 7) [*Kang and Polvani, 2011; Davis and Birner,*  
 150 *2017; Waugh et al., 2018; Solomon et al., 2016*]. Not only are most of the correlations not  
 151 significant, the sign of relationship changes from negative to positive depending on the  
 152 season. Note that the strength of the HC is also poorly correlated with the STJ latitude  
 153 and the sign of correlation is inconsistent over seasons. (Fig. 3, row 4).

154 In contrast, the STJ strength has a consistently weak to moderate negative correla-  
 155 tion with the HC edge (Fig. 3, row 2) for all seasons and both hemispheres. This relation-  
 156 ship is strongest in the Northern Hemisphere (NH). Likewise, the correlation between the  
 157 strength of the HC and the strength of the STJ is weakly positive (Fig. 3, row 3), which  
 158 is true for all seasons except the near-zero negative value of NH's summer (JJA). These  
 159 results suggest that a weaker, more poleward HC is associated with a weaker STJ. Such a  
 160 conclusion is also consistent with the patterns shown in Fig. 2b-c where for the Southern  
 161 Hemisphere (SH), a poleward expansion of the HC edge by  $\approx 1.2^\circ$  is associated with a  
 162 weakening of the HC by about  $0.5 \times 10^{10} \text{ kg s}^{-1}$  and a weakening of the STJ by  $0.8 \text{ m s}^{-1}$ .

163 The fifth and sixth rows of Fig. 3 show the correlations between strength and loca-  
 164 tion for the STJ and for the HC, and in both cases there are moderate negative correla-  
 165 tions except during summer in both hemispheres and fall in the NH. Thus during winter  
 166 and spring the STJ is weaker when it is further poleward and the HC is weaker when ex-  
 167 panded.

168 Although not examined in detail, we note that there is a similar weak relationship  
 169 between the STJ and EDJ, where the STJ and EDJ latitudes are not correlated and there  
 170 is a small negative correlation between the EDJ latitude and STJ strength in the NH. The  
 171 lack of correlations between the latitudes of the STJ and EDJ has been shown previously

[Solomon *et al.*, 2016; Davis and Birner, 2017; Waugh *et al.*, 2018], and correlations between metrics of the jets are shown in Figure S2 of the Supporting Information.

#### 4 Forced Response

Next, we examine the response of the HC and STJ to an instantaneous quadrupling of atmospheric CO<sub>2</sub>. The multi-model annual-mean response of the zonal-mean meridional circulation, zonal wind, and temperature are shown in the right hand plots of Figure 2. Here, the response was calculated by averaging the fields over years 100-150 of the 4xCO<sub>2</sub> simulation and subtracting the climatological annual-mean values taken from the piControl simulation. As shown previously [e.g., Held and Soden, 2006; Lu *et al.*, 2007; Frierson *et al.*, 2007], there is an expansion and weakening of HC in response to the increase in CO<sub>2</sub> (in the SH, the multi-model mean  $\phi HC$  moves poleward by 1.7° and  $maxHC$  decreases by up to  $1.1 \times 10^{10} \text{ kg s}^{-1}$ ). There is also a slight poleward shift of the Ferrel cells (Fig. 2d), and in the SH, this shift of the Ferrel cell is accompanied by a  $1.6 \text{ m s}^{-1}$  strengthening and 2.9° poleward shift of the EDJ (Fig. 2e), again consistent with previous studies [e.g., Kushner *et al.*, 2001; Barnes and Polvani, 2013; Simpson *et al.*, 2014; Collins *et al.*, 2013]. There is additionally a strong increase in zonal winds in the subtropical upper troposphere, resulting in a strengthening of the STJ in both hemispheres ( $4.6 \text{ m s}^{-1}$  in the SH,  $1.6 \text{ m s}^{-1}$  in the NH). Finally, Fig. 2f shows the well-known warming of the entire troposphere, with amplified warming in the tropical upper troposphere and polar lower troposphere.

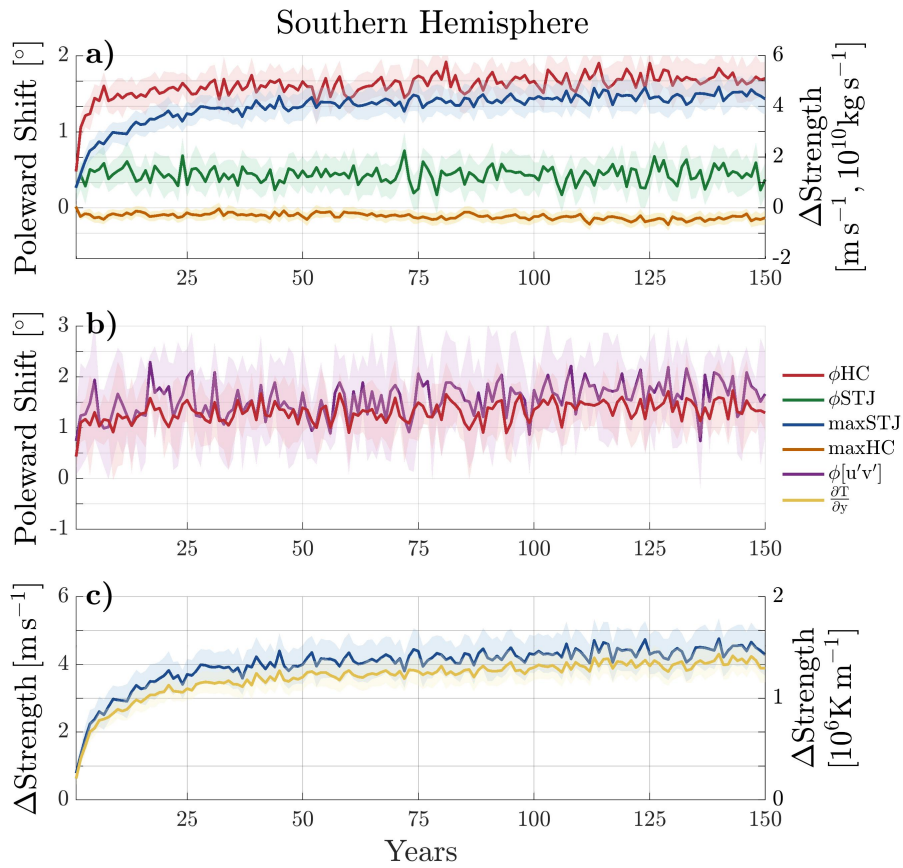
Comparison of the left and right hand side of Figure 2 shows the same general relationship between the HC and EDJ for the cases of natural variability and 4xCO<sub>2</sub>, that is a more poleward EDJ occurs with an expanded and weaker HC. There is, however, a change in relationship between the HC and tropical upper tropospheric fields, such that a weaker STJ and colder tropical upper troposphere is associated with an expanded HC interannually but the opposite occurs for 4xCO<sub>2</sub>. This change of relationship is consistent with the well documented difference in the HC and EDJ response to ENSO forcing and global warming: the HC widens and EDJ moves poleward under global warming but during ENSO warming, the HC contracts and EDJ moves equatorward [Lu *et al.*, 2008]. Figure 2 shows that the differing response between ENSO and global warming does not occur for the STJ as it strengthens both interannually (i.e., in response to ENSO warming), and under global warming. Shaw and Tan [2018] present these same broad conclusions,

204 explaining that the STJ responds to forcing that occurs in the tropics whereas the HC and  
 205 EDJ responses are dominated by subtropical forcing.

206 Figure 2 shows the multi-model responses to  $4xCO_2$ , but it is also of interest to con-  
 207 sider the response of individual models. There is a poleward expansion of the HC and  
 208 increase in the STJ strength for all models and both hemispheres, but the sign of change  
 209 in the STJ latitude varies between models, especially in the NH where STJ moves equa-  
 210 torward in a similar number of models as it does poleward (see Supporting Information,  
 211 Figure S3). However, although there is consistent sign change in  $\phi_{HC}$  and  $\max STJ$ , there  
 212 is an insignificant correlation across models in the magnitude of the change ( $r \approx 0.2$ ). This  
 213 indicates that the models with a larger change in  $\phi_{HC}$  do not necessarily have a larger  
 214 change in  $\max STJ$ , which is inconsistent with the interannual correlation. Also, while  
 215 there is no consistency across the models in direction of change in  $\phi_{STJ}$ , there is a pos-  
 216 itive correlation between the changes in  $\phi_{HC}$  and  $\phi_{STJ}$  across models ( $r \approx 0.4 - 0.5$ ), so  
 217 models with large poleward shift in  $\phi_{HC}$  tend to have a larger shift in  $\phi_{STJ}$ .

218 The inconsistency in sign of the response or weak correlations across models be-  
 219 tween STJ metrics and  $\phi_{HC}$  suggests that different processes are responsible for the changes  
 220 in the STJ and HC (see further discussion below). Note, this contrasts the consistencies  
 221 between the HC edge and EDJ latitude responses. In all models there is a poleward move-  
 222 ment of  $\phi_{HC}$  and  $\phi_{EDJ}$  in response to  $4xCO_2$ , there is a high correlation in the  $\phi_{HC}$  and  
 223  $\phi_{EDJ}$  response across models, and the slope of the linear fit between change across mod-  
 224 els is close to the multi-model mean regression coefficient for interannual variations in the  
 225 piControl runs (see Figure 8 of *Waugh et al. [2018]*). This consistency occurs interannu-  
 226 ally and in response to forcing, strongly suggesting that the latitudes of the HC edge and  
 227 EDJ are governed by the same physical processes.

233 Previous studies have demonstrated that examining the transient response in the  
 234  $4xCO_2$  simulations provides insight into the processes involved [*Grise and Polvani, 2017*;  
 235 *Chemke and Polvani, 2019*]. Following these studies we show in Figure 4a the evolution of  
 236 the multi-model annual-mean time series of the metrics in the SH (shading represents the  
 237 95th percentile between models). Consistent with Fig. 2d-f, the HC weakens slightly (or-  
 238 ange) and shifts poleward  $\approx 1.7^\circ$  (red), while the STJ strengthens by  $4.6 m s^{-1}$  (blue) and  
 239 shifts minimally (green). Interestingly, the shift of the HC and strengthening of the STJ  
 240 occur on different timescales. Following *Grise and Polvani [2017]*, we calculate a quan-



228 **Figure 4.** Time series of Southern Hemispheric response to quadrupling atmospheric  $\text{CO}_2$  for (a) the HC  
 229 edge (red) and strength (orange) and the STJ location (green) and strength (blue), (b) the latitude of maximum  
 230 eddy momentum flux (purple) compared to the HC edge (red), and (c) the STJ strength (blue) compared to the  
 231 maximum meridional temperature gradient (yellow) between  $0\text{--}45^\circ\text{S}$ . For each plot, shading represents the  
 232 95% confidence interval of model spread.

241 tity's response time as the time it takes to reach 90% of its steady state value (averaged  
242 over years 140-150). The HC edge responds in 7 years while the STJ does so in 40 years.  
243 For comparison, the global-mean surface temperature increases even more slowly, taking  
244 around 65 years to reach 90% of its value at 150 years [Grise and Polvani, 2017; Chemke  
245 and Polvani, 2019; Seviour et al., 2018].

246 These broad conclusions, that  $4xCO_2$  induces a rapid poleward shift of the HC edge  
247 and slower strengthening of the STJ, also hold in the NH (see Supporting Information,  
248 Fig. S4). The major difference between hemispheres is that in the NH, the STJ initially  
249 shifts poleward and then returns to its original latitude by the end of the first century  
250 [Shaw and Voigt, 2015]. Additionally, the metrics' behavior is generally consistent across  
251 all seasons where the HC shifts poleward and weakens slightly, and the STJ strengthens  
252 and shifts minimally.

253 We now consider the physical processes associated with these changes in the HC  
254 and STJ. Chemke and Polvani [2019] showed that the rapid expansion of the HC occurs  
255 with increases in the subtropical static stability and a poleward shift in the subtropical  
256 eddy momentum fluxes. This connection is presented in Fig. 4b which shows the evo-  
257 lution of  $\phi_{HC}$  (red) and the latitude of the maximum eddy momentum fluxes (purple)  
258 for the subset of models that archived the necessary daily fields (indicated in Supporting  
259 Information, Table S1) to calculate the eddy momentum fluxes (see Chemke and Polvani  
260 [2019] for details of the calculation). Both fields in Fig. 4b increase at a similar rapid  
261 time scale. Further, they have similar year-to-year variations with a model-mean correla-  
262 tion of about 0.6 for both hemispheres in the piControl time series.

263 As the strength of the STJ ( $maxSTJ$ ) increases much more slowly than the shift in  
264  $\phi_{HC}$  or eddy momentum fluxes, it must be dynamically related to other processes. One  
265 possibility is that meridional temperature gradients, and thus thermal wind balance, sets  
266  $maxSTJ$  [Davis and Birner, 2017]. To test this we examine the evolution of the maxi-  
267 mum meridional temperature gradient calculated at each latitude between  $0-45^\circ S$  (Fig. 4c,  
268 yellow). There is good agreement in the evolution of  $maxSTJ$  and the meridional tem-  
269 perature gradient, as both increase on the same time scale, which is slower than  $\phi_{HC}$  but  
270 quicker than the global mean surface temperature. Furthermore, there is not a significant  
271 change in the latitude of maximum meridional temperature gradient, consistent with the  
272 limited movement of the STJ (not shown).

273 The close connections between  $\phi_{HC}$  and the latitude of the maximum eddy momen-  
274 tum fluxes and between  $maxSTJ$  and maximum meridional temperature gradient are also  
275 found for the spread among models: Models with larger shift in latitude of the maximum  
276 eddy momentum fluxes in response to  $4xCO_2$  tend to have a larger shift in  $\phi_{HC}$  (correla-  
277 tion of 0.97 in the SH) and models with larger increase in meridional temperature gradient  
278 tend to have larger increase in  $maxSTJ$  (correlation of 0.91 in the SH). This further in-  
279 dicates that while the movement of the HC edge is connected to the shifts in latitude of  
280 maximum eddy momentum flux, a strengthening of the STJ is accompanied by changes in  
281 the meridional temperature gradient.

## 282 5 Concluding Remarks

283 Although the STJ latitude does not co-vary interannually with the HC edge [Davis  
284 and Birner, 2016; Solomon et al., 2016; Waugh et al., 2018], we have shown that the HC  
285 edge is weakly to moderately correlated to the STJ strength. However, this correlation  
286 does not hold when the two features respond to  $4xCO_2$ . On interannual time scales the  
287 STJ tends to be weaker with a wider HC, whereas the STJ strengthens and the HC widens  
288 under increased  $CO_2$ .

289 The distinct time scales of response to increased  $CO_2$  by the HC width and STJ  
290 strength indicate that the two features are influenced by different physical processes. As  
291 shown in Section 4, the rapid expansion of the HC is associated with a poleward shift  
292 in the subtropical eddy momentum fluxes. Both the edge of the HC and the subtropical  
293 eddy fields are strongly impacted by subtropical baroclinicity and shift poleward given  
294 an increase in static stability (see Chemke and Polvani [2019] for details). However, the  
295 strength of the STJ shows no connection to the eddy momentum fluxes, and the slower  
296 time scale of the STJ's strengthening is instead associated with increases in the meridional  
297 temperature gradient in the subtropical upper troposphere. This is in agreement with the  
298 suggestion by Davis and Birner [2017] that the differences between movement of the HC  
299 edge and the STJ are due to the meridional stream function (used to define the HC edge)  
300 being physically linked to the distribution of eddy momentum fluxes via subtropical baro-  
301 clinicity, whereas the upper tropospheric winds (used to define the STJ) are related to the  
302 latitudinal distribution of temperature.

303           The differing sensitivities of the HC and STJ to changes in eddy momentum fluxes  
304 may also explain the change in sign of the HC and STJ relationship between interannual  
305 variability and the forced response. As discussed above, the interannual variability resem-  
306 bles that due to ENSO [e.g., *Lu et al.*, 2008], and the differences between HC response  
307 from interannual variability and 4xCO<sub>2</sub> are the same as for ENSO versus global warm-  
308 ing. Previous studies have linked the different HC responses between ENSO and global  
309 warming to the width of the warming and its impact on eddies [*Sun et al.*, 2013; *Tandon*  
310 *et al.*, 2013]. *Sun et al.* [2013] showed, using an idealized model, that the zonally sym-  
311 metric response to tropical warming is a contraction of HC and equatorward shift of EDJ  
312 for both narrow or broad warming, but when waves were included the mid-latitude eddy  
313 response and feedbacks caused an expansion of HC and poleward movement of EDJ for  
314 broad warming (but not for narrow warming). Irrespective of whether there is a mid lati-  
315 tude eddy response there is a strengthening of the STJ for tropical warming. Thus the sign  
316 of the HC and STJ relationship varies between interannual variability, or narrow warming,  
317 and increased CO<sub>2</sub>, a broader warming.

318           The above hypothesis that the STJ is much less sensitive than the HC to changes  
319 in mid-latitude eddies requires continued examination. An obvious approach to test this  
320 is through idealized modeling, similar to the work of *Sun et al.* [2013] and *Tandon et al.*  
321 [2013]. Both studies have shown that the change in response of the HC and EDJ to nar-  
322 row, ENSO-like warming and broad, global warming can be reproduced in dynamical core  
323 simulations while also allowing for isolation of the role of eddies and feedbacks. Our next  
324 objective is to use similar idealized simulations to further investigate the relationships be-  
325 tween the HC and STJ, and their dynamical connections to eddy momentum fluxes and  
326 temperature gradients.

## Acknowledgments

The CMIP5 data used in this study are freely available through the Earth System Grid Federation (<https://esgf-node.llnl.gov>). We acknowledge the World Climate Research Programme's Working Group on Coupled Modelling, which is responsible for CMIP, and we thank the climate modeling groups for producing and making available their model output. M. E. M. and D. W. W. are partially supported by NSF award FESD-1338814 from the U.S. National Science Foundation (NSF). K. M. G. is supported in part by NSF award AGS-1522829

## References

- Adam, O., K. M. Grise, P. Staten, I. R. Simpson, S. M. Davis, N. A. Davis, D. W. Waugh, T. Birner, and A. Ming (2018), The tropd software package (v1): standardized methods for calculating tropical-width diagnostics, *Geoscientific Model Development*, *11*(10), 4339–4357.
- Archer, C. L., and K. Caldeira (2008), Historical trends in the jet streams, *Geophysical Research Letters*, *35*(8).
- Barnes, E. A., and L. Polvani (2013), Response of the midlatitude jets, and of their variability, to increased greenhouse gases in the cmip5 models, *Journal of Climate*, *26*(18), 7117–7135.
- Chemke, R., and L. M. Polvani (2019), Exploiting the abrupt 4× co2 scenario to elucidate tropical expansion mechanisms, *Journal of Climate*, *32*(3), 859–875.
- Collins, M., R. Knutti, J. Arblaster, J.-L. Dufresne, T. Fichefet, P. Friedlingstein, X. Gao, W. J. Gutowski, T. Johns, G. Krinner, et al. (2013), Long-term climate change: projections, commitments and irreversibility.
- Davis, N., and T. Birner (2016), Climate model biases in the width of the tropical belt, *Journal of Climate*, *29*(5), 1935–1954.
- Davis, N., and T. Birner (2017), On the discrepancies in tropical belt expansion between reanalyses and climate models and among tropical belt width metrics, *Journal of Climate*, *30*(4), 1211–1231.
- Eichelberger, S. J., and D. L. Hartmann (2007), Zonal jet structure and the leading mode of variability, *Journal of Climate*, *20*(20), 5149–5163.
- Frierson, D. M., J. Lu, and G. Chen (2007), Width of the hadley cell in simple and comprehensive general circulation models, *Geophysical Research Letters*, *34*(18).

- 359 Fu, Q., and P. Lin (2011), Poleward shift of subtropical jets inferred from satellite-  
360 observed lower-stratospheric temperatures, *Journal of climate*, *24*(21), 5597–5603.
- 361 Grise, K. M., and L. M. Polvani (2017), Understanding the time scales of the tropospheric  
362 circulation response to abrupt co<sub>2</sub> forcing in the southern hemisphere: Seasonality and  
363 the role of the stratosphere, *Journal of Climate*, *30*(21), 8497–8515.
- 364 Held, I. M., and A. Y. Hou (1980), Nonlinear axially symmetric circulations in a nearly  
365 inviscid atmosphere, *Journal of the Atmospheric Sciences*, *37*(3), 515–533.
- 366 Held, I. M., and B. J. Soden (2006), Robust responses of the hydrological cycle to global  
367 warming, *Journal of climate*, *19*(21), 5686–5699.
- 368 Kang, S. M., and L. M. Polvani (2011), The interannual relationship between the latitude  
369 of the eddy-driven jet and the edge of the hadley cell, *Journal of Climate*, *24*(2), 563–  
370 568.
- 371 Kim, H.-k., and S. Lee (2004), The wave–zonal mean flow interaction in the southern  
372 hemisphere, *Journal of the atmospheric sciences*, *61*(9), 1055–1067.
- 373 Kushner, P. J., I. M. Held, and T. L. Delworth (2001), Southern hemisphere atmospheric  
374 circulation response to global warming, *Journal of Climate*, *14*(10), 2238–2249.
- 375 Lachmy, O., and N. Harnik (2014), The transition to a subtropical jet regime and its main-  
376 tenance, *Journal of the Atmospheric Sciences*, *71*(4), 1389–1409.
- 377 Lee, S., and H.-k. Kim (2003), The dynamical relationship between subtropical and eddy-  
378 driven jets, *Journal of the atmospheric sciences*, *60*(12), 1490–1503.
- 379 Lu, J., G. A. Vecchi, and T. Reichler (2007), Expansion of the hadley cell under global  
380 warming, *Geophysical Research Letters*, *34*(6).
- 381 Lu, J., G. Chen, and D. M. Frierson (2008), Response of the zonal mean atmospheric cir-  
382 culation to el niño versus global warming, *Journal of Climate*, *21*(22), 5835–5851.
- 383 Manney, G. L., and M. I. Hegglin (2018), Seasonal and regional variations of long-term  
384 changes in upper-tropospheric jets from reanalyses, *Journal of Climate*, *31*(1), 423–448.
- 385 Matthews, A. J., and G. N. Kiladis (1999), The tropical–extratropical interaction between  
386 high-frequency transients and the madden–julian oscillation, *Monthly weather review*,  
387 *127*(5), 661–677.
- 388 Otkin, J. A., and J. E. Martin (2004), The large-scale modulation of subtropical cyclogene-  
389 sis in the central and eastern pacific ocean, *Monthly weather review*, *132*(7), 1813–1828.
- 390 Ryoo, J.-M., Y. Kaspi, D. W. Waugh, G. N. Kiladis, D. E. Waliser, E. J. Fetzer, and  
391 J. Kim (2013), Impact of rossby wave breaking on us west coast winter precipitation

- 392 during enso events, *Journal of Climate*, 26(17), 6360–6382.
- 393 Seviour, W. J., S. M. Davis, K. M. Grise, and D. W. Waugh (2018), Large uncertainty in  
394 the relative rates of dynamical and hydrological tropical expansion, *Geophysical Re-*  
395 *search Letters*, 45(2), 1106–1113.
- 396 Shaw, T., and A. Voigt (2015), Tug of war on summertime circulation between radiative  
397 forcing and sea surface warming, *Nature Geoscience*, 8(7), 560.
- 398 Shaw, T. A., and Z. Tan (2018), Testing latitudinally dependent explanations of the circu-  
399 lation response to increased co2 using aquaplanet models, *Geophysical Research Letters*,  
400 45(18), 9861–9869.
- 401 Shepherd, T. G., and C. McLandress (2011), A robust mechanism for strengthening of  
402 the brewer–dobson circulation in response to climate change: Critical-layer control of  
403 subtropical wave breaking, *Journal of the Atmospheric Sciences*, 68(4), 784–797.
- 404 Simpson, I. R., T. A. Shaw, and R. Seager (2014), A diagnosis of the seasonally and lon-  
405 gitudinally varying midlatitude circulation response to global warming, *Journal of the*  
406 *Atmospheric Sciences*, 71(7), 2489–2515.
- 407 Solomon, A., L. Polvani, D. Waugh, and S. Davis (2016), Contrasting upper and lower  
408 atmospheric metrics of tropical expansion in the southern hemisphere, *Geophysical Re-*  
409 *search Letters*, 43(19).
- 410 Sun, L., G. Chen, and J. Lu (2013), Sensitivities and mechanisms of the zonal mean atmo-  
411 spheric circulation response to tropical warming, *Journal of the Atmospheric Sciences*,  
412 70(8), 2487–2504.
- 413 Tandon, N. F., E. P. Gerber, A. H. Sobel, and L. M. Polvani (2013), Understanding hadley  
414 cell expansion versus contraction: Insights from simplified models and implications for  
415 recent observations, *Journal of Climate*, 26(12), 4304–4321.
- 416 Taylor, K. E., R. J. Stouffer, and G. A. Meehl (2012), An overview of cmip5 and the ex-  
417 periment design, *Bulletin of the American Meteorological Society*, 93(4), 485–498.
- 418 Wang, N., D. Jiang, and X. Lang (2018), Metric-dependent tendency of tropical belt width  
419 changes during the last glacial maximum, *Journal of Climate*, 31(20), 8527–8540.
- 420 Waugh, D. W., K. M. Grise, W. J. Seviour, S. M. Davis, N. Davis, O. Adam, S.-W. Son,  
421 I. R. Simpson, P. W. Staten, A. C. Maycock, et al. (2018), Revisiting the relationship  
422 among metrics of tropical expansion, *Journal of Climate*, 31(18), 7565–7581.
- 423 Webster, P. J., and J. R. Holton (1982), Cross-equatorial response to middle-latitude forc-  
424 ing in a zonally varying basic state, *Journal of the Atmospheric Sciences*, 39(4), 722–

425 733.

426 Winters, A. C., and J. E. Martin (2014), The role of a polar/subtropical jet superposition  
427 in the may 2010 nashville flood, *Weather and Forecasting*, 29(4), 954–974.

428 Zhang, W., and G. Villarini (2018), Uncovering the role of the east asian jet stream and  
429 heterogeneities in atmospheric rivers affecting the western united states, *Proceedings of*  
430 *the National Academy of Sciences*, 115(5), 891–896.